Molecular Vision 2020; 26:623-640 <http://www.molvis.org/molvis/v26/623>
Received 14 April 2020 | Accepted 31 August 2020 | Published 2 September 2020

Alterations in proteome of human sclera associated with primary open-angle glaucoma involve proteins participating in regulation of the extracellular matrix

Elena N. Iomdina,[1] Natalya K. Tikhomirova,[2] Alexander M. Bessmertny,[1] Marina V. Serebryakova,[2] Viktoriia E. Baksheeva,[2] Arthur O. Zalevsky,[3,4,5] Vladislav I. Kotelin,[1] Olga A. Kiseleva,[1] Sbrui M. Kosakyan,[1] Andrey A. Zamyatnin Jr.,[2,5] Pavel P. Philippov,[2] Evgeni Yu. Zernii[2,5]

[1]Helmholtz National Medical Research Center of Eye Diseases, Moscow, Russia; [2]Belozersky Institute of Physico-Chemical Biology, Lomonosov Moscow State University, Moscow, Russia; [3]Faculty of Bioengineering and Bioinformatics, Lomonosov Moscow State University, Moscow, Russia; [4]Shemyakin and Ovchinnikov Institute of Bioorganic Chemistry of the Russian Academy of Sciences, Moscow, Russia; [5]Institute of Molecular Medicine, Sechenov First Moscow State Medical University, Moscow, Russia

Purpose: Primary open-angle glaucoma (POAG) is a common ocular disease, associated with abnormalities in aqueous humor circulation and an increase in intraocular pressure (IOP), leading to progressive optical neuropathy and loss of vision. POAG pathogenesis includes alterations of the structural properties of the sclera, especially in the optic nerve head area, contributing to the degeneration of the retinal ganglion cells. Abnormal sclera biomechanics hinder adequate compensation of IOP fluctuations, thus aggravating POAG progression. The proteomic basis of biomechanical disorders in glaucomatous sclera remains poorly understood. This study is aimed at revealing alterations in major scleral proteins, associated with POAG, at different stages of the disease and with different IOP conditions.

Methods: Samples of sclera were collected from 67 patients with POAG during non-penetrating deep sclerectomy and from nine individuals without POAG. Scleral proteins were extracted with a strong lysis buffer, containing a combination of an ionic detergent, a chaotropic agent, and a disulfide reducing agent, and were separated using sodium dodecyl sulfate–polyacrylamide gel electrophoresis (SDS–PAGE). The major scleral proteins were selected, subjected to in-gel digestion, and identified using matrix-assisted laser desorption ionization-time of flight mass spectrometry (MALDI-TOF)/TOF mass spectrometry (MS), coupled with tandem mass spectrometry (MS/MS). The specific POAG-associated alterations of the selected proteins were analyzed with SDS–PAGE and confirmed with western blotting of the scleral extracts, using the respective antibodies. The group of POAG-associated proteins was analyzed using Gene Ontology and genome-wide association study enrichment and protein–protein interaction network prediction.

Results: A total of 11 proteins were identified, among which six proteins, namely, vimentin, angiopoietin-related protein 7, annexin A2, serum amyloid P component, serum albumin, and thrombospondin-4, were found to be upregulated in the sclera of patients with advanced and terminal POAG. In the early stages of the disease, thrombospondin-4 level was, on the contrary, reduced when compared with the control, whereas the concentration of vimentin varied, depending on the IOP level. Moreover, angiopoietin-related protein 7 manifested as two forms, exhibiting opposite behavior: The common 45 kDa form grew with the progression of POAG, whereas the 35 kDa (apparently non-glycosylated) form was absent in the control samples, appeared in patients with early POAG, and decreased in concentration over the course of the disease. Functional bioinformatics analysis linked the POAG-associated proteins with IOP alterations and predicted their secretion into extracellular space and their association with extracellular vesicles and a collagen-containing extracellular matrix.

Conclusions: POAG is accompanied by alterations of the scleral proteome, which represent a novel hallmark of the disease and can reflect pathological changes in scleral biochemistry and biomechanics. The potential mechanisms underlying these changes relate mainly to the structure of the extracellular matrix, protein glycosylation, and calcium binding, and may involve fibroblast cytoskeleton regulation, as well as oxidative and inflammatory responses.

Open-angle glaucoma is a severe ocular disease, characterized by the altered balance of aqueous humor (AH) production from the ciliary body and its outflow, through the trabecular meshwork (TM) and the uveoscleral pathway, resulting in an increased individual level of intraocular pressure (IOP) and progressive optical neuropathy. The latter includes damage to the retinal ganglion cells (RGCs) and excavation of the optic nerve head (ONH; so-called cupping), and ultimately, leads to irreversible loss of visual function.

Correspondence to: Evgeni Yu. Zernii, Laboratory of visual reception, Belozersky Institute of Physico-Chemical Biology, Lomonosov Moscow State University, 1-40 Leninskye gory, Moscow 119992, Russia; Phone: +74959392344; FAX: +74959390338; email: zerni@belozersky.msu.ru

The most frequent, primary open-angle glaucoma (POAG), represents idiopathic disease, whereas secondary forms of open-angle glaucoma are commonly induced by iatrogenic factors, such as the administration of corticosteroids or antineoplastic agents [1,2]. Despite etiological variability, different types of open-angle glaucoma share pathogenic mechanisms. Consistently, the data on these mechanisms can be obtained from animal models of the iatrogenic disease (such as a model of corticosteroid-induced glaucoma) and studies involving patients with POAG [3-5]. Although considerable efforts have been made to understand the pathophysiology of glaucoma and the development of new methods for its diagnosis and treatment, this disease still occupies a significant position among the causes of poor vision and blindness worldwide [2,6].

Generally, POAG is recognized as a multifactorial disease, affected by several metabolic, functional (such as altered ocular blood flow), genetic, and environmental factors, as well as aging [7,8]. Biochemically, POAG can be related to mitochondrial dysfunction, oxidative stress, and immune response [9-11]. Three key mechanisms of glaucomatous RGC damage have been proposed. The first two mechanisms consider direct damage to axons in the lamina cribrosa (with interruption of axonal transport) and excitotoxicity as the main triggers of RGC apoptosis [12,13]. The third mechanism, suggested in recent years, relies on aberrations of the structural and biomechanical features of the corneoscleral membrane [14-18]. Apparently, such changes stem from increased disorganization of the connective tissue structures of the anterior and posterior components of the eye [19,20]. The disturbance of structural properties of the sclera, especially in the ONH area, may lead to RGC degeneration [17,21,22]. Furthermore, the inability of the corneoscleral membrane to respond normally to the deformation hinders adequate compensation of IOP fluctuations, thus further aggravating POAG progression [18,23,24].

Alterations in the biomechanical properties of the corneoscleral membrane in the glaucomatous eye can be caused by biochemical abnormalities, such as alterations in the protein composition of the scleral connective tissue in the drainage zone (i.e., in aqueous humor (AH) outflow pathways) and the ONH area. Among these abnormalities are changes in the extracellular matrix (ECM), associated with the aberrant metabolism of collagen, the major structural protein of sclera and lamina cribrosa [18,25]. POAG progression is accompanied by an increase in the content and level of the cross-linking of Type I collagen in the sclera, which negatively impacts the biomechanical properties of this tissue and leads, for instance, to its increased rigidity [15,18,26,27]. IOP-induced remodeling of the collagen structure results in a stiffer pressure strain response of the sclera in glaucoma [18]. Meanwhile, information regarding the participation of other, non-collagenous proteins in POAG-associated alterations in the ECM and fibroblasts, constituting scleral connective tissue [18], remains scarce. Studies have reported aberrations in sclera biomechanics and the accompanying changes in the proteomes of the sclera and the TM in various animal models of the disease [28-32]. Thus, changes in the protein content were found in the TM of glaucomatous mice, where, along with the accumulation of collagen Type IV and I, there was an increase in the concentration of fibronectin and elastin [31]. Furthermore, direct proteomic analysis of the sclera of glaucomatous mice revealed elevated levels of several molecules involved in integrin-linked kinase signaling and actin cytoskeleton signaling pathways (myosin, spectrin, actinin, vimentin, and α-smooth muscle actin), as well as fluctuations in the content of several other proteins [32]. However, in human studies, POAG-related proteomic perturbations were examined only for the TM [33,34] and the retina [35], whereas possible changes in the protein content of the glaucomatous sclera have never been addressed.

In this study, by using an extensive cohort of patients undergoing surgical treatment of POAG and individuals without POAG, we examined alterations of the scleral proteome (focusing on the major proteins of this tissue) at different stages of the disease and under different IOP conditions. Using a combination of mass-spectrometric and immunological techniques, we identified six proteins exhibiting significant changes in the sclera of patients with POAG and analyzed them using Gene Ontology (GO) enrichment, genome-wide association studies (GWASs) enrichment, and protein–protein interaction (PPI) network prediction. The results provide new insight into the biochemical mechanisms of POAG, which could facilitate the development of effective treatment of the disease.

METHODS

Materials: Rabbit polyclonal antibodies against human vimentin (cat. # MBS3013681), angiopoietin-related protein 7 (cat. # MBS9414699), annexin A2 (cat. # MBS9414682), serum amyloid P component (cat. # MBS2002237), and thrombospondin-4 (cat. # MBS8241709), as well as goat anti-rabbit (cat. # MBS128200) and anti-mouse (cat. # MBS539266) immunoglobulin G (IgG) peroxidase conjugates, were from MyBioSource, Inc (San Diego, CA). Mouse monoclonal antibodies against human glyceraldehyde-3-phosphate dehydrogenase (GAPDH) were kindly provided by Prof. V.I. Muronetz (Lomonosov Moscow State University) [36].

Prestained protein standards and mass spectrometry (MS)-grade trypsin protease were from Thermo Fisher Scientific, Inc (Waltham, MA). Other chemicals were from Sigma (St. Louis, MO), Amresco (St. Louis, MO), or Serva (Heidelberg, Germany) and were at least reagent grade.

Human subjects: The study involved a total of 67 patients with POAG receiving surgical treatment at Helmholtz National Medical Research Center of Eye Diseases (Moscow, Russia). The detailed demographic characteristics and comorbidities of the participants are summarized in Appendix 1. Before the operation, the patients were monitored and treated for at least 2 years. They received maximum complex hypotensive therapy according to the generally accepted protocol for POAG treatment, including prostaglandin analogs, beta-blockers, and carbonic anhydrase inhibitors. All individuals were examined at least once every 3 months with IOP measurements performed in the morning (9–10 AM) under epibulbar anesthesia using the conventional Goldmann tonometry method. At presentation, the attending ophthalmologists assigned the patients to POAG stages II, III, and IV in accordance with national glaucoma guidelines [37]. Stage II (moderate POAG) is changes in the visual fields in the paracentral section in combination with its narrowing by more than 10° in the upper or lower nasal segments or both; regional optic disc cupping in some places reaches the disc edge. Stage III (advanced POAG) is a concentrically narrowed visual field, which is less than 15° from the fixation point in at least one segment; subtotal optic disc cupping reaches the disc edge. Stage IV (severe or terminal POAG) is complete loss of visual acuity and visual fields or preservation of light perception with the wrong projection or a small islet of the visual field in the temporal sector; total optic disc cupping occurs. The patients in each group were additionally assigned to grade A, B, or C depending on their IOP conditions: A, IOP ≤21 mmHg, B, IOP of 22–28 mmHg, and C, IOP ≥29 mmHg. The control group included nine individuals without history of POAG deceased from trauma or acute heart failure (Table 1). The control individuals were employed as eye donors for keratoplasty, and according to their records, before death, they had been ophthalmologically healthy. All human studies were conducted in accordance with Declaration of Helsinki, under approval of the local ethical committee of Helmholtz National Medical Research Center of Eye Diseases and in adherence to the ARVO statement on human subjects.

Collection of scleral samples and preparation of extracts: All patients with POAG underwent non-penetrating deep sclerectomy, aimed at increasing AH outflow and reducing IOP. During the operation, tissue samples were obtained from the anterior region of the scleral membrane according to the standard protocol [38]. Approximately 1 mm^2 avascular fragments of sclera were selected, excised, rinsed with PBS (1X; 140 mM NaCl, 2.68 mM KCl, 10 mM Na_2HPO_4, 1.8 mM KH_2PO_4, pH 7.45; Thermo Fisher Scientific), placed in 1.5 ml plastic tubes with 50 mM Tris-HCl buffer (pH 6.8), 9 M urea, 4.3% sodium dodecyl sulfate (SDS), and 7.5% β-mercaptoethanol (lysis buffer) [39,40], and frozen at −70 °C. The control samples were obtained from cadaveric eyes that were delivered to the operating room, on average, within 24 h postmortem. During this period, the eyes were stored in small tightly closed boxes without solution at +4 °C, and before the surgery, the eyes were treated with chloramphenicol. Scleral samples of the same size were excised from the same region and treated exactly as described above. For protein extraction, the samples were thawed, diluted 1:2 with the same buffer, and homogenized using Teflon homogenizer (ten passes). Protein extracts from each sclera sample were separated from the precipitates with centrifugation at 39,000 ×*g* for 20 min at 4 °C and stored at −70 °C.

Identification of scleral proteins: The scleral protein extracts were subjected to SDS–polyacrylamide gel electrophoresis (SDS–PAGE) with staining with Coomassie brilliant blue R-250. The amount of the protein in each SDS–PAGE track was adjusted according to the total protein concentration evaluated using the BCA Protein Assay Kit (Thermo Fisher Scientific, Inc.) or using GAPDH as a loading control normalized in the parallel western blotting experiment. The selected protein bands were excised from the gel, washed with 40% acetonitrile and 0.05 M NH_4HCO_3, and dehydrated in acetonitrile. The proteins were subjected to in-gel digestion using 15 µg/ml MS-grade trypsin in 0.05 M NH_4HCO_3 at 37 °C overnight. The resulting peptides were extracted with 0.5% trifluoroacetic acid and mixed on a steel target with 20 mg/ml 2,5-dihydroxybenzoic acid in 20% (v/v) acetonitrile with 0.5% (v/v) trifluoroacetic acid, and subjected to mass spectrometry analysis. Peptide mass fingerprints were obtained using ultrafleXtreme MALDI-TOF/TOF mass spectrometer (Bruker Daltonics, Billerica, MA) equipped with a Smartbeam-II laser (Nd:YAG, 355 nm) in reflector mode. Monoisotopic [MH]+ molecular ions were detected in the 600–5,000 m/z range with a peptide tolerance of 30 ppm. MS/MS spectra of certain peptides were obtained in Lift mode of the instrument within 1 Da accuracy for daughter ion measurements. The mass spectra were analyzed using flexAnalysis 3.3 software (Bruker Daltonics). Protein identification was performed using Mascot software (Matrix Science, Boston, MA) and the NCBI protein database with permitting of one missed cleavage, Met oxidation, and Cys-propionamide. Scores exceeding 80 were considered statistically significant ($p<0.05$).

Molecular Vision 2020; 26:623-640 <http://www.molvis.org/molvis/v26/623>

Table 1. Characteristics of control and POAG groups.

Parameter		Control	POAG stage					
			IIA	IIB	IIIB	IIIC	IVC	Total
Number of participants		9	12	11	21	19	4	67
Mean age ± SD, years*		46.55±10.21	66.17±8.11	66.27±8.22	70.00±7.76	64.05±9.81	72.50±10.34	67.16±8.83
Gender, %**	Male	55.6	76.7	45.5	38.1	47.4	50	47.8
	Female	44.4	33.3	54.5	61.9	52.6	50	52.2
IOP ± SD, mmHg		-	20.0±0.95	24.8±2.8	25.2±3.1	32.1±1.9	35.3±3.9	-
Refraction abnormalities, %	Myopia***	-	8.3	18.2	9.5	21.05	-	13.4
	Hyperopia	-	-	-	-	10.5	-	3.0
Comorbidities, %	Arterial hypertension	55.55	75.0	54.5	85.7	57.9	75.0	70.1
	Coronary heart disease	55.55	41.7	36.4	76.2	26.3	25.0	46.3
	Diabetes mellitus	-	-	18.2	14.3	10.5	-	10.4

* No significant age differences between glaucoma groups (p=0.119); ** No significant gender differences between all groups (p=0.605); *** No significant correlation with POAG stage (R=0.21; p=0.320).

Quantification of scleral proteins: The content of the selected proteins in the sclera extracts was verified using western blotting (SDS–PAGE in 15% resolving gel, followed by protein transfer to nitrocellulose membrane [41]). The membranes were incubated for 1.5 h with 10% delipidated dry milk in PBS, containing 0.05% v/v Tween-20 (PBST). The protein bands were stained with overnight incubation of the membranes with the respective rabbit polyclonal antibodies (1:1,000 in PBST). The membranes were rinsed three times with PBST and incubated for 1.5 h with goat anti-rabbit IgG peroxidase conjugate (1:1,500 in PBST). Then, the membranes were rinsed with PBST again, and the protein bands were visualized in the ChemiDoc™ XRS+ gel documentation system (Bio-Rad, Hercules, CA) using the enhanced chemiluminescence (ECL) kit SuperSignal™ West Dura Extended Duration Substrate (Thermo Fisher Scientific, Inc.). The weight fractions of the scleral proteins were estimated from the SDS–PAGE or western blotting experiments or both with densitometric scanning of the bands and data analysis using GelAnalyzer v.2010a software.

Bioinformatics: The group of POAG-associated scleral proteins was analyzed using the GO Ontology database and the Protein ANalysis THrough Evolutionary Relationships (PANTHER) Classification System. Gene enrichment was performed in three categories: biologic process, molecular function, and cellular component. The data were corrected employing the false discovery rate (FDR) or Bonferroni correction. Terms with a p value of less than 0.05 and a minimum count of 3 were collected and grouped into clusters based on their membership similarities. In addition, pathways (using BioPlanet 2019 and Kyoto Encyclopedia of Genes and Genomes [KEGG] 2019) and diseases or drugs (using GWAS Catalog 2019 and UK Biobank GWAS v1) enrichment was performed with Enrichr. The term hits were sorted by p value ranking.

Potential PPIs were analyzed using the Search Tool for the Retrieval of Interacting Genes (STRING) under the default settings. The PPI network was constructed considering a combined interaction score of >0.4.

Statistical analysis: The data were analyzed with the mean standard error (SE) method. Mean scores, SEs, and statistical significance were calculated with SigmaPlot 11 (SYSTAT Software, San Jose, CA). Statistical significance was evaluated with an unpaired two-tailed *t* test (for comparisons of two groups), one-way analysis of variance (ANOVA, for multiple comparisons), and Pearson's chi-square test (for analyzing the categorical data). A p value of less than 0.05 was considered statistically significant.

RESULTS

Characteristics of the experimental groups: The study involved 67 patients with POAG and nine individuals with no history of glaucoma, deceased on account of various reasons (Table 1, Appendix 1). The selected cohort of patients did not contain individuals with normal tension glaucoma. All patients were assigned to stages II–IV of POAG, depending on the severity of the patients' visual field loss. Thus, individuals with moderate POAG (Stage II) were characterized by changes in the paracentral section of the visual field, which narrowed by more than 10° in the nasal hemifield. In patients with advanced POAG (Stage III), the visual field was concentrically narrowed, being less than 15° from the fixation in at least one segment. Patients with Stage IV (severe or terminal) POAG had completely lost visual acuity or preserved light perception with the wrong projection or had a small islet of the visual field in one of the temporal sectors. In addition, patients who presented with stages II–IV of POAG exhibited different optic disc states: regional (Stage II), subtotal (Stage III), or total (Stage IV) optic disc cupping. Finally, to account for the associated changes in IOP, patients with each stage of POAG were additionally assigned to grade A (IOP ≤21 mmHg), B (IOP of 22–28 mmHg), or C (IOP ≥29 mmHg). Based on these criteria, all 67 patients were divided into five POAG groups: IIA, IIB, IIIB, IIIC, and IVC (Table 1, Appendix 1). The number of participants and the demographic parameters of the POAG groups were generally similar, thus enabling a reasonable comparison between them. An exception was group IVC (terminal POAG), which was substantially smaller than the other groups, as such patients were rare, due to the infrequency of their surgical treatment. All POAG groups contained similar numbers of men and women (on average, 48% male), with a mean age of 67 ± 9.0 years (Table 1). Some of the patients with glaucoma (13%) had refractive abnormalities. In addition, patients with glaucoma exhibited a high prevalence of arterial hypertension (70%) and coronary heart disease (46%), and some had diabetes mellitus (10%).

Identification of the major proteins of the human sclera: To compare protein profiles of sclera at different stages of POAG and under different IOP conditions, we used fragments of this tissue, collected from individuals with POAG (during non-penetrating deep sclerectomy) and from individuals without POAG (postmortem) for use as an absolute control. The protein extracts of the sclera (usually 60–80 µg of the total protein) were obtained using a strong lysis buffer, containing a combination of an ionic detergent, a chaotropic agent, and a disulfide reducing agent (for details, see Methods). The proteomic extracts obtained from all control and POAG

samples were first monitored with one-dimensional SDS–PAGE. Figure 1 shows representative protein profiles of the non-glaucomatous sclera, as well as the sclera of patients with Stage III glaucoma, which were most widely represented in the cohort. Each track contained the same amount of total protein (10 µg). As can be seen, all samples were characterized by qualitatively similar patterns containing nine major bands (Figure 1A). Using in-gel trypsin digestion and MALDI-TOF peptide mass fingerprinting, bands 4, 5, 6, 7, and 9 were recognized as serum amyloid P component (APCS or SAP), annexin A2 (ANXA2), angiopoietin-related protein 7 (ANGPTL7), vimentin (VIM), and serum albumin (ALB; Figure 1B). Band 1 contained a mixture of hemoglobin subunits alpha and beta, whereas band 2 corresponded to histone H2A. These proteins were detected with analysis of at least two characteristic bands with relatively high methodological quality (score >80), except histone H2A, identification of which was verified with MS/MS analysis (Appendix 2).

In addition to these findings, SDS–PAGE analysis of certain extracts of glaucomatous and non-glaucomatous sclera revealed an extra band 3 corresponding to a protein of 23–24 kDa (Figure 1A). Using mass spectrometry analysis, this protein was identified as fibrinogen alpha chain (Figure 1B). As the molecular weight of the latter is approximately 95 kDa, we suggested that band 3 corresponded to the proteolytic fragment of the protein. Consistently, the respective tryptic hydrolysate contained only peptides, covering approximately the first quarter of the fibrinogen alpha sequence (Appendix 3). Furthermore, certain sclera samples contained extra proteins 8 and 10 with molecular weights of approximately 56 and 108 kDa, respectively (the approximate positions of these bands are denoted in Figure 1A), which were identified as fibrinogen beta chain and collagen alpha-1 (VI) chain (COL6A1; Figure 1B). The identification of fibrinogen alpha and COL6A1 was confirmed with MS/MS analysis (Appendix 2).

Primary analysis of POAG-associated alterations in the major proteins of the human sclera: The quantitative analysis of the SDS–PAGE data for all control and POAG samples revealed that the concentration of hemoglobin and histone H2A did not differ reliably among control individuals and patients with POAG (Appendix 4), whereas fibrinogen alpha, fibrinogen beta, and COL6A1 were found only occasionally in the sclera samples (Figure 1A). Meanwhile, the concentration of VIM, ANGPTL7, ANXA2, and APCS seemed to become higher in POAG. This trend was more visible when the amount of the protein in each SDS–PAGE track was adjusted using GAPDH as a loading control (Figure 2A). The concentration of the four sclera proteins described above exhibited apparent growth with progression of the disease. Interestingly, under such experimental conditions, a similar tendency was observed for ALB (Figure 2A). Thus, analysis of the SDS–PAGE data indicated a two- to threefold increase in the scleral concentration of ALB during the later stages of POAG (Figure 2B).

In this case, we managed to detect an extra band 11 with molecular weight >170 kDa (Figure 2A). Notably, the concentration of this protein in the sclera extracts was higher during the later stages of POAG. Using mass spectrometry analysis, band 11 was identified as thrombospondin-4 (THBS4). Electrophoretic mobility of band 11 (>170 kDa) was beyond the expected molecular weight of THBS4 (about 106 kDa). However, MS/MS analysis confirmed the correct identification of this protein (Appendix 2). The apparent difference in molecular weights was attributed to different levels of THBS4 glycosylation [42]. Overall, APCS, ANXA2, ANGPTL7, VIM, ALB, and THBS4 were considered candidate proteins, undergoing specific changes in POAG.

Verification of POAG-associated alterations in the major proteins of the human sclera: Whereas the POAG-associated elevation of the scleral content of ALB was reliably evident from SDS–PAGE, the alterations in the concentration of VIM, ANGPTL7, ANXA2, APCS, and THBS4 were less obvious and therefore, were verified with western blotting of all control and POAG samples, using the respective antibodies and GAPDH as a loading control (Figure 3A). The patterns of some of these proteins differed from those observed in SDS–PAGE. Thus, in the case of APCS and ANXA2 we detected major bands of about 25 and 38 kDa, respectively, which corresponded to the molecular weights of their polypeptides. The position of the VIM band also correlated with its expected molecular weight (53 kDa), although in some cases we observed staining of additional non-specific bands. Meanwhile, THBS4 appeared mainly as the 140 kDa band, whereas the band of >170 kDa, observed in SDS–PAGE (see Figure 1 and Figure 2) manifested as a minor form of the protein. Finally, ANGPTL7 always manifested as two specific bands with molecular weights of about 35 kDa and about 45 kDa, which apparently correspond to non-glycosylated and glycosylated forms of the protein, respectively [43].

Generally, in the late stages of POAG the concentration of VIM, ANGPTL7, ANXA2, APCS, and THBS4 in the sclera was higher in comparison with that of the controls (Figure 3A), which agreed with the SDS–PAGE data (see Figure 2). However, only ANXA2 and APCS demonstrated gradual growth along with an increase in severity of the disease (Figure 3B). The concentration of VIM (Figure 3B) in early

A

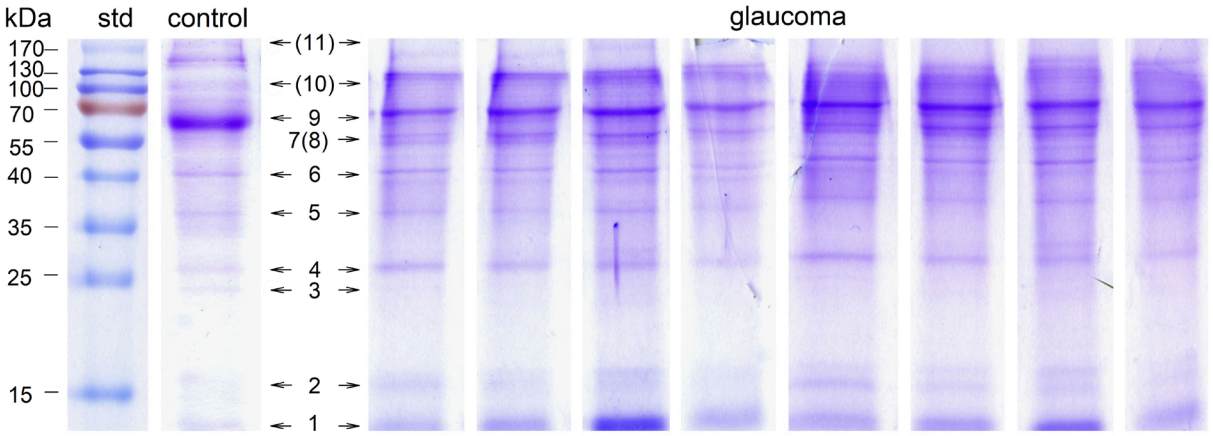

B

#	ID	Mr (Da)	UniProt	Score	Pept	Cov	Method
1	Hemoglobin subunit alpha	15248	P69905	76	6	49%	MS
	Hemoglobin subunit beta	15988	P68871	86	7	59%	MS
2	Histone H2A	14225	Q96QV6	79	3	15%	MS, MS/MS
3	Fibrinogen alpha (fragm)	94914	P02671	103	9	-	MS, MS/MS
4	Serum amyloid P-component	25371	P02743	128	7	27%	MS
5	Annexin A2	38580	P07355	88	12	36%	MS
6	Angiopoietin-related protein 7	39993	O43827	122	13	32%	MS
7	Vimentin	53619	P08670	101	18	42%	MS
8	Fibrinogen beta	55892	P02675	225	27	48%	MS
9	Serum albumin	69321	P02768	123	24	35%	MS
10	Collagen alpha-1(VI)	108462	P12109	52	12	16%	MS, MS/MS
11	Thrombospondin-4	105802	P35443	130	11	12%	MS, MS/MS

Figure 1. Identification of the major proteins of normal and POAG human sclera. **A**: Representative sodium dodecyl sulfate–polyacrylamide gel electrophoresis (SDS–PAGE) images of protein extracts obtained from non-glaucomatous sclera (control) and sclera of different patients with Stage IIIB primary open-angle glaucoma (POAG; glaucoma). Each track contains 10 µg of total protein. Protein standards in kDa (track std) are denoted in the left column. The positions of the bands corresponding to the major sclera proteins are indicated with arrows (the approximate positions of bands 8, 10, and 11 are indicated in parentheses). **B**: The results of identification of the protein bands indicated in panel **A**, using tryptic peptide mass fingerprinting (matrix assisted laser desorption ionization-time of flight [MALDI-TOF] mass spectrometry [MS]) and tandem mass spectrometry (MS/MS) of the peptides. Molecular weights (Mr) and accession numbers (UniProt) of the proteins, the identification scores (Score), and the number of detected peptides (Pept) and sequence coverage data in % (Cov) are provided.

POAG exhibited an inverted correlation, with the IOP level elevated at Stage IIA (normal IOP) but returned to the baseline level at Stage IIB (high IOP). In contrast, the 140 kDa band of THBS4 decreased in patients with stages IIA and IIB of POAG (Figure 3B). However, in advanced glaucoma (stages IIIB through IVC), the concentration of these proteins gradually increased with augmentation of the overall severity of the disease. Interestingly, two forms of ANGPTL7 exhibited opposite POAG-associated alterations (Figure 3B). Thus, the concentration of its 45 kDa (glycosylated) form increased

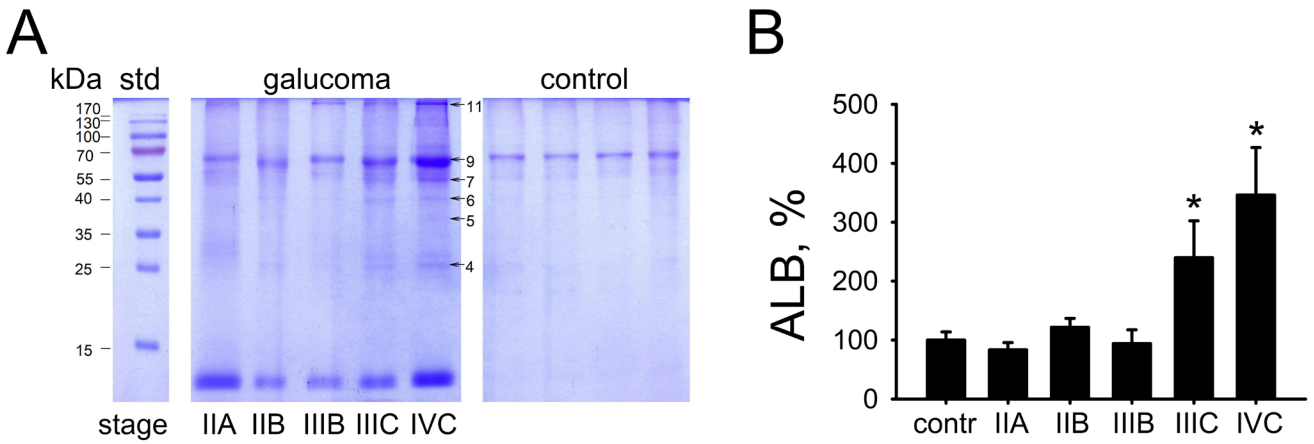

Figure 2. Determination of POAG-associated alterations in the content of the major proteins of the human sclera. **A**: Representative sodium dodecyl sulfate–polyacrylamide gel electrophoresis (SDS–PAGE) images of protein extracts obtained from non-glaucomatous sclera (control) and sclera of patients with different stages of primary open-angle glaucoma (POAG; glaucoma). The amount of the total protein in each track is adjusted using glyceraldehyde-3-phosphate dehydrogenase (GAPDH) as a loading control in parallel western blotting experiments (not shown). Protein standards in kDa (track std) are denoted in the left column. Arrows indicate six proteins (the protein numbers are the same as in Figure 1) exhibiting altered content in the sclera of the patients with POAG. **B**: The weight fractions of serum albumin (ALB) estimated from the SDS–PAGE data obtained for control individuals (100%) and the patients with different stages of POAG. *p<0.05 compared to the values obtained for the control group.

along with POAG progression. In contrast, the 35 kDa (non-glycosylated) variant of the protein was absent in the sclera of the control individuals, yet appeared in relatively high quantities in patients with Stage IIA, and the concentration decreased over the course of the disease.

Functional bioinformatics analysis of POAG-associated proteins of the human sclera: All identified proteins were divided into two groups. The first group included proteins similarly distributed in control and glaucomatous tissue (hemoglobin alpha and beta and histone H2A) or occasionally found in the sclera samples (fibrinogen alpha and beta). The second (POAG) group contained proteins exhibiting a prominent increase in the patients with glaucoma (VIM, ANGPTL7, ANXA2, APCS, ALB, and THBS4). Although in this study we did not obtain reliable evidence of POAG-associated alterations in scleral collagen, we observed its elevation in POAG in previous studies [15,26]. Therefore, for further analysis, COL6A1 was attributed to the POAG group, which thus contained a total of seven proteins.

To predict the common biologic activities of the POAG-associated proteins identified, they were subjected to GO enrichment in three categories, cellular component, biologic process, and molecular function, using the GO Ontology database. Processes involving at least three of the identified proteins were considered. The most significant enrichment was observed in the category cellular component pointing to the extracellular character of the proteins (Figure 4A). Thus, all seven candidates reliably fell into the subcategories extracellular region and extracellular space, six (except ANGPTL7) could be attributed to extracellular organelle, extracellular vesicle, and extracellular exosome, whereas three proteins (THBS4, ANXA2, and APCS) corresponded to extracellular matrix and collagen-containing extracellular matrix. Importantly, the use of additional data improvement tools, such as the FDR or Bonferroni correction, did not change the observed clustering. Enrichment in the category biologic process gave less reliable hits (Figure 4B), among which only response to stimulus included all seven proteins, probably indicating their common ability to undergo secretion into the extracellular space. The most significant category involving five of the seven proteins was negative regulation of developmental process, and it was the only hit left upon FDR correction. Pathways enrichment, performed using two alternative sources (BioPlanet 2019 and KEGG 2019), revealed that, according to the p value ranking, two proteins (COL6A1 and THBS4) are implicated in ECM–receptor interactions (Appendix 5).

Enrichment in the category molecular function highlighted the common ability of the identified proteins to bind metal cations, especially calcium, and to participate in protein–protein interactions (Figure 4C). Remarkably, PPI analysis revealed that all the proteins, except ANGPTL7, could be integrated in the single interaction network (Figure 4D). Furthermore, this network may contain two additional

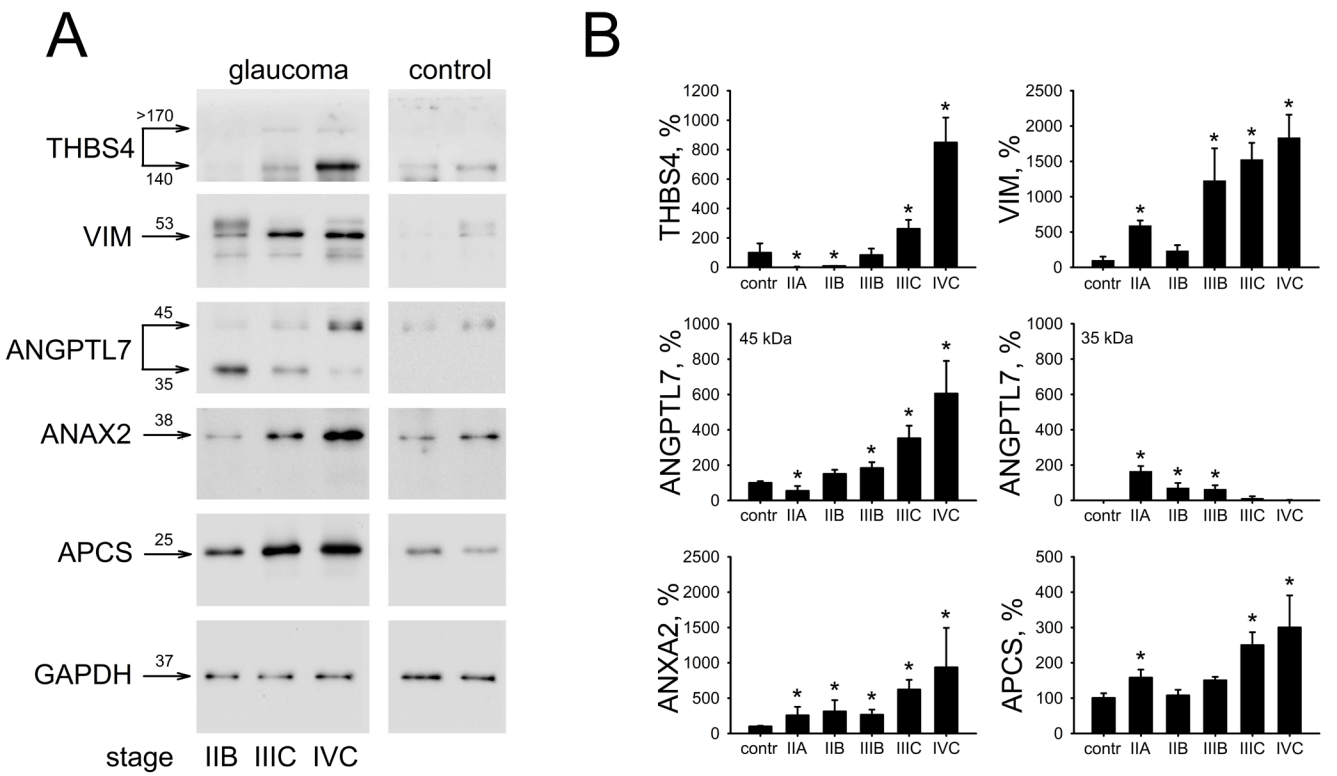

Figure 3. Verification of POAG-associated alterations in the content of the major proteins of the human sclera. **A**: Representative western blotting images of thrombospondin-4 (THBS4), vimentin (VIM), angiopoietin-related protein 7 (ANGPTL7), annexin A2 (ANXA2), and serum amyloid P component (APCS) in protein extracts obtained from non-glaucomatous sclera (control) and sclera of patients with different stages of primary open-angle glaucoma (POAG; glaucoma). The amount of the total protein in each track is adjusted using glyceraldehyde-3-phosphate dehydrogenase (GAPDH) as a loading control. Arrows indicate apparent molecular weights (in kDa) of the proteins. **B**: The weight fractions of the scleral proteins estimated from the western blotting data obtained for control individuals (100%) and patients with different stages of POAG. *p<0.05 compared to the values obtained for the control group. The actual p values for all pairwise comparisons are given in Appendix 7.

Ca^{2+}-binding proteins, alpha-2-HS-glycoprotein and S100A10. In the resulting network, three functional clusters could be distinguished, which include ALB/APCS, ANXA2/VIM, and THBS4/COL6A1. Given that ANGPTL7 was previously implicated in the regulation of collagen expression [43], this protein was included in the third cluster, containing components of the collagen–ECM system.

Finally, the potential pathological activities of the POAG-associated proteins were assessed by performing an enrichment analysis of GWASs. Interestingly, the search in two of the sources (GWAS Catalog 2019 and UK Biobank GWAS v1) revealed significant relationships between three proteins, ANGPTL7, COL6A1, and THBS4, with intraocular pressure and refraction abnormalities (Appendix 6).

DISCUSSION

This study is the first to address stage- and IOP-dependent changes in the proteome of the human sclera, accompanying the development of POAG in patients. However, there are specific conditions related to the content of the experimental groups and methodology employed in the study that should be considered before making any interpretations of the data obtained. First, these are specific demographic parameters and comorbidities of the patients with POAG. Although there were no significant gender differences between the control and glaucoma groups, the patients with POAG were generally older than the control individuals (eye donors for keratoplasty; Table 1). There were no statistically significant differences in age between the patients of the glaucoma groups. Because the most of the observed proteomic effects reliably correlated with the stage of POAG, we concluded that they were associated with progression of the disease, but

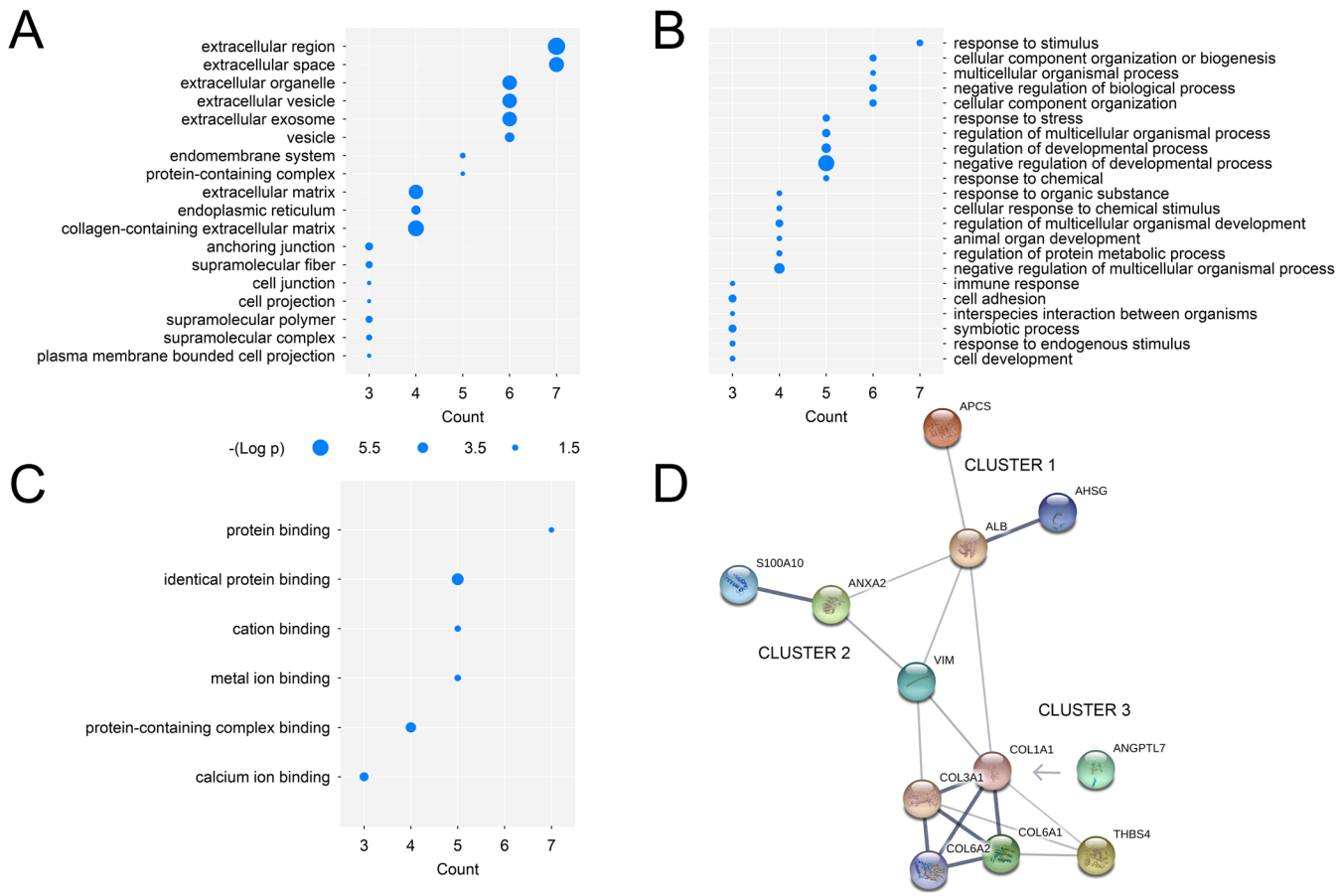

Figure 4. Functional bioinformatics analysis of POAG-associated proteins of the human sclera. **A**–**C**: Visualization of Gene Ontology (GO) enrichment analysis performed using the Protein ANalysis THrough Evolutionary Relationships (PANTHER) categories cellular component (**A**), biologic process (**B**), and molecular function (**C**). **D**: Protein–protein interactions (PPI) network built using STRING. All nodes are characterized by a combined interaction score of >0.4. In addition to the analyzed proteins, the network includes the following potential contributors: alpha-2-HS-glycoprotein (AHSG), S100-A10 protein, collagen alpha-1(I) chain (COL1A1), collagen alpha-1(III) chain (COL3A1), and collagen alpha-2(VI) chain (COL6A2).

not the age-related changes. Some of the patients with glaucoma (approximately 13%) had been diagnosed with myopia. However, we detected no reliable correlation between myopia and POAG in the experimental groups. This was especially true as four out of nine patients did not have axial (true) but had refractive myopia caused by incipient cataract. Thus, the described proteomic alterations in the sclera of patients with POAG cannot be attributed to refractive abnormalities.

The second set of conditions includes principles underlying POAG diagnosis and assignment of the patients to a particular experimental group, as well as their treatment characteristics. The cohort contained only individuals who were characterized by severe progression of the disease as they required surgical intervention. Before the operation, all patients were monitored and treated for at least 2 years with examinations once every 2–3 months. At presentation, the attending ophthalmologist considered the dynamic changes in individually tolerated IOP (in all patients, IOP was measured under similar conditions with respect to the time of day, anesthesia, and other factors), perimetric indices, and optic nerve state. The grouping of the patients was performed based on such complex symptomatology recorded during their prolonged management. Thus, each POAG group might be considered as a whole, and the search for correlations between the changes in the sclera proteome and individual parameters of the disease (such as IOP) ignoring other aspects of the patient's state is not entirely justified. Notably, all patients received maximum complex hypotensive therapy, which included as acting substances prostaglandin analogs, beta-blockers, and carbonic anhydrase inhibitors. Although we cannot rule out the impact of this drug therapy on sclera metabolism, the therapy was identical in all POAG groups,

which makes their comparison relevant. The presence of pronounced proteomic differences between the glaucoma groups suggests that these differences were associated with glaucoma progression rather than caused by antiglaucoma therapy.

The third set of conditions is related to the methods of collection and analysis of the scleral samples. Although biochemical examination of the posterior sclera is of special interest, this study dealt with fragments of anterior sclera, as it was the only material available from the patients. The collection of sclera in the posterior pole (the optic nerve region) is not provided for by any antiglaucoma intervention except eye enucleation in patients with painful terminal glaucoma. However, analysis of the anterior region of this tissue is also important with respect to pathogenesis of POAG, because this zone participates in AH outflow, one of the key factors in the development of the disease. In addition, despite the known heterogeneity of the scleral membrane, the metabolic and structural responses may be similar in various regions of this tissue. Thus, the POAG-associated increase in rigidity is characteristic not only of the posterior but also of the anterior sclera [44].

Notably, in the scleral samples we analyzed we used the semiproteomic approach focusing on the most represented proteins of the tissue, which were chosen based on one-dimensional SDS–PAGE, identified with MALDI mass spectrometry, and quantified with western blotting. Therefore, the minor POAG-dependent proteins in the sclera remained outside the scope of this study. In addition, there were several major scleral proteins that cannot be extracted from the tissue using this approach (a combination of an ionic detergent, a chaotropic agent, and a disulfide reducing agent) and therefore, remained outside the scope of this study. For instance, proper determination of alterations in scleral collagen requires completely different methods for sample preparation and analysis, such as colorimetric determination of hydroxyproline upon complete acidic hydrolysis of the protein [15,26].

Generally, 11 proteins made up the bulk of the sclera extracts obtained from patients with glaucoma and control individuals, which accords with previous proteomic studies of normal sclera [45]. Several proteins were either similarly distributed in the control and glaucomatous samples (hemoglobin alpha and beta and histone H2A) or occasionally found in the extracts (fibrinogen alpha and beta). Hemoglobin and fibrinogen represent major plasma proteins, whereas histone H2A is a ubiquitous nuclear component, expressed in multiple eukaryotic cells. The absence of significant changes in the content of these common plasma and tissue components indicates that the control and POAG scleral samples were generally similar in structure, vasculature, and other parameters.

The potential POAG-associated proteins included VIM, ANGPTL7, ANXA2, APCS, ALB, and THBS4 as well as COL6A1. Interestingly, all represent partially or permanently extracellular proteins. The sclera is mostly composed of ECM, built from lamellae of collagen, elastin, and proteoglycans, and only approximately 20% of this tissue consists of cellular lamellae, containing scleral fibroblasts responsible for the production of ECM components [18,46]. Thus, aberrations in the scleral proteins that constitute and regulate the ECM may represent one of the critical factors underlying abnormal scleral biomechanics associated with glaucoma. This suggestion is well supported by the results of the functional bioinformatics analysis (see Figure 4). Thus, they not only linked all of the proteins above to IOP alterations and indicated their colocalization in extracellular space but also predicted the association of some of them (COL6A1, THBS4, ANXA2, and APCS) with collagen-containing ECM. THBS4, ANXA2, and APCS were recognized as Ca^{2+}-binding proteins, which is important, because calcium is implicated in ECM assembly and binds to many ECM proteins [47]. In addition, according to GO enrichment in the category biologic process, five proteins (THBS4, ANGPTL7, ANXA2, VIM, and APCS) contribute to the regulation of development, which is known to be closely associated with ECM remodeling [48]. Consistently, pathways enrichment, performed using KEGG, revealed that THBS4 and COL6A1 are directly implicated in ECM–receptor interactions. These findings accord with the generated PPI network that consisted of three main clusters (see Figure 4E), one of which, alongside COL6A1, contained THBS4 and most likely ANGPTL7, which are known to participate in the regulation of the ECM–collagen system (see below).

Increased ECM deposition in the TM, leading to IOP elevation, is one of the most recognized biochemical mechanisms in glaucoma [49]. THBS4 is a common ECM protein, previously found in the TM and the sclera [32,50,51]. Thrombospondins are Ca^{2+}-binding glycoproteins that reside in the ECM, where they interact with collagens as well as fibronectin, integrins, and other non-collagenous ECM proteins, and contribute to collagen fibril assembly [42]. Pentameric THBS4 functions as an adaptor protein in ECM assembly by coordinating its components, such as integrin, laminin, fibronectin, and collagens I, II, III, and V. Consistently, THBS4 deficiency results in the formation of disorganized collagen fibrils and an increased number of fibrils of a larger diameter in tissues [52]. Alterations in THBS4 could contribute to eye

diseases associated with ECM changes, such as POAG [18]. There are multiple reports implicating THBS4 in glaucoma pathogenesis. It was hypothesized that AH outflow can be hindered by an accumulation of certain proteins in this eye liquid, continuously liberating from its pathway tissues [53,54]. THBS4 is one such protein: It is released from the TM and uveoscleral structures and can contribute to the outflow resistance [51,55]. Interestingly, ex vivo experiments with anterior segments of the human eye, perfused at 11 mmHg pressure, demonstrated that the THBS4 concentration in the sclera dropped with a decrease in the AH outflow [55]. In the meantime, in a similar ex vivo study, conducted under higher pressure conditions (17.6 mmHg), the THBS4 concentration in the TM was fourfold higher in its low-flow regions in comparison with its high-flow regions [50]. These data correlate with the present findings, indicating that THBS4 is downregulated in the sclera in the early stages of POAG (Stage II, moderate IOP elevations) and becomes significantly upregulated at the advanced disease stage (stages IIIC and IVC, pronounced IOP elevations). Consistently, the level of another thrombospondin, TBSP1, increases in the sclera of mice with glaucoma [32]. It is known that in glaucomatous sclera, collagen is less organized, while exhibiting an increase in the number and cross-sectional area of the fibrils [27,56]. THBS4 and TBSP5 were suggested to prevent collagen helices from abnormal modification and cross-linking [57]. Based on the present data, we can speculate that in the early stages of POAG, a decrease in THBS4 results in collagen disorganization and consequently, a reduced outflow capacity of the sclera and the TM. Meanwhile, in the later stages of the disease, the compensatory increase in THBS4 expression may lead to the release of this protein into AH, thus further hindering the circulation.

Abnormal ECM regulation may constitute the pathological effect of another protein, ANGPTL7 (also known as corneal derived transcript 6, CDT6), representing glycosylated protein found in the cornea, TM, and sclera [43,58-60]. This protein is extensively produced and secreted by TM cells in response to glaucomatous stimuli, such as dexamethasone treatment, and its concentration is increased in the AH of patients with POAG [60-62]. Furthermore, ANGPTL7 is found to modulate the ECM of the TM. Thus, the overexpression or silencing of ANGPTL7 in TM cells altered production of crucial ECM proteins, such as collagens, namely, Type I, IV, and V, as well as myocilin, versican, and MMP1. In addition, ANGPTL7 contributed to the response of the ECM to steroids, which promote IOP elevation in glaucoma [63]. Finally, increased expression of ANGPTL7 induces collagen and proteoglycan deposition [43]. The present study is the first to detect the pronounced growth of ANGPTL7 in the sclera of patients with POAG. We suggest that this effect, together with alterations in the THBS4 concentration, can contribute to perturbations in the scleral ECM associated with glaucoma.

In addition, in the sclera of patients with POAG, ANGPTL7 was detected as two bands with molecular weights of approximately 35 and 45 kDa. Based on the human gene sequence, the molecular weight of the protein is expected to be 38 kDa. As ANGPTL7 contains predicted N-glycosylation sites, the 45 kDa band was previously recognized as its glycosylated form [43]. Given these data, we suggest that the 35 kDa represents the non-glycosylated form of ANGPTL7. Interestingly, this form was detected exclusively in patients with POAG, but its fraction was reduced with progression of the disease, representing a novel hallmark of glaucoma. This observation accords with the fact that global protein glycosylation is altered in glaucomatous tissues [64].

The second cluster of POAG-associated proteins includes ANXA2 and VIM (see Figure 4D). Among these proteins, only the Ca^{2+}-binding protein ANXA2 was previously suggested to contribute to POAG pathogenesis via a direct effect on the ECM, which concurs with the results of the present GO enrichment studies. Thus, ANXA2 mediates the interaction of fibronectin-containing exosomes with heparan sulfate in the ECM of the TM, which is necessary for ensuring the normal cell–matrix interactions and AH outflow. Consistently, in dexamethasone-induced glaucoma, the accumulation of pathological ECM deposits is accompanied by a significant reduction of ANXA2 in the exosomes [65]. Given these findings, we propose that the moderate growth of this protein in the sclera, seen in the present study in the late stages of POAG, represents a compensatory response aimed at promoting the remodeling of this tissue.

Yet another highly probable effect of ANAX2, as well as VIM, in glaucoma could be related to their intracellular role in maintaining the cytoskeleton of scleral fibroblasts. POAG is associated with an increased AH level of the soluble CD44 receptor, which upregulates IOP levels and acts on TM cells by decreasing the expression of ANXA2 and increasing its phosphorylation [66]. These modifications may impact the regulatory activity of ANXA2 toward actin growth and motility, resulting in increased formation of actin spokes and cross-linked networks (CLANs) in the TM, associated with glaucoma [66,67]. CLANs are suggested to contribute to the resistance of AH outflow and elevated IOP, by generating stiffer TM cells and tissue [67]. A similar effect may be realized in glaucomatous sclera, as it is characterized by the increased activation of actin cytoskeleton and integrin signaling pathways, evidence of which has been found in

experiments performed on animal models of the disease [32]. Thus, the changes in the content of ANXA2, seen in the sclera of patients with POAG, may represent a mechanism aimed at recovery from alterations in the cytoskeleton, associated with glaucoma. In addition, the described regulatory activity of ANAX2 may be realized with the participation of another Ca^{2+}-binding protein, S100A10, which was suggested by the present PPI analysis (see Figure 4D). This protein was previously detected in healthy human sclera [45], and the protein is known to form a stable heterotetrameric complex with ANAX2, which binds to F-actin and regulates its bundling. Animal studies of glaucoma also revealed an increase in the sclera content of VIM [32], another cytoskeleton protein, comprising the intermediate filaments. We consistently observed pronounced upregulation of VIM in the sclera of patients at an advanced stage of POAG. VIM is a common component of fibroblasts, is known to protect cells against compressive stress, and preserves their mechanical integrity by enhancing their elasticity [68]. Thus, VIM upregulation in the sclera represents an appropriate response of VIM fibroblasts to increased IOP conditions in the later stages of POAG. In addition, VIM functions as a promoter of wound healing; targeting of this protein in the TM was suggested to reduce scarring in glaucoma filtration surgery [69]. Interestingly, VIM is secreted by activated macrophages, thus participating in the immune function [70]. Given the nonuniform character of VIM elevation in POAG, observed in the present study, a spike in the VIM concentration in the early stages of the disease could be related to inflammatory responses, which are found to contribute to glaucoma pathogenesis [10].

The third cluster of POAG-associated proteins contains secreted plasma-derived components, ALB and APCS, as well as alpha-2-HS-glycoprotein that was suggested by the PPI analysis (see Figure 4D). In contrast to the other plasma proteins that remained unchanged in POAG, ALB and APCS were clearly upregulated in the sclera of patients with glaucoma (see Figure 3). Similarly, the level of alpha-2-HS-glycoprotein was elevated in glaucomatous AH [71]. ALB was previously found to be increased in the glaucomatous retina, which apparently represents antioxidant protection of this tissue [72]. In POAG, oxidative damage is known to impact several eye tissues, such as the retina, trabecular meshwork, and cornea [72-74], and may affect the sclera. For instance, alterations in intrinsic antioxidant protection were shown to correlate with low corneal and apparently, sclera hysteresis, associated with POAG [75,76]. Thus, ALB elevation may represent the response of the sclera to oxidative stress associated with POAG. Consistently, ALB together with APCS was detected among stress-response proteins in the GO enrichment analysis in the category biologic process (see Figure 4B). Serum proteins, mainly ALB, were suggested to be continuously released into the AH from its outflow pathway tissues, thus hampering the outflow [53,54]. The AH of patients with POAG is characterized by an increased ALB level [77]. We speculate that upregulation of scleral ALB, observed in the present study, could contribute to the abnormal protein content of AH that hinders its circulation and exacerbates POAG.

APCS is an acute-phase glycoprotein belonging to the pentraxin family [78]. It is known to bind to amyloid deposits and protect them from proteolytic degradation, thus contributing to the pathogeneses of amyloidoses, including Alzheimer's disease (AD) [79,80]. In early studies, increased APCS concentration was detected in pseudoexfoliative material collected from patients with glaucoma [81]. Growing evidence indicates that neurodegenerative processes in glaucoma and AD possess multiple similarities [82,83]. Patients with AD are characterized by a high occurrence of glaucoma [84], and POAG progression may be directly related to the level of β-amyloid and tau protein in the cerebrospinal fluid of the respective individuals [85]. Furthermore, glaucoma is associated with alterations in well-recognized AD biomarkers in various eye tissues and liquids. These alterations include increased levels of amyloid precursor protein, β-amyloid and phosphorylated tau protein in the retina [83,86-88], a decreased level of β-amyloid, and an increased level of tau protein in the vitreous humor [89], an increased level of serum amyloid A in the trabecular meshwork and serum [90], as well as increased levels of ApoAI, ApoCIII, ApoE, transthyretin, and α2M in the aqueous humor [91]. In this context, the increased level of APCS in the sclera of patients with POAG represents another important feature implicating this tissue in the AD-like pathogenesis of glaucoma. Whether APCS is increased in the glaucomatous retina remains to be investigated, but we suggest that in this case, it could stabilize β-amyloid deposits found in RGCs [83], thus contributing to the pathogenesis of the disease. Interestingly, APCS is known to decrease neutrophil binding to extracellular matrix components, which explains its association with the ECM–collagen system, revealed in the present functional bioinformatics analysis (see Figure 4A). Furthermore, APCS is capable of restraining fibrocyte activation and therefore, has been trialed as a potential antiscarring therapeutic in photorefractive keratectomy and glaucoma filtration surgery [92-94]. The present data indicated that such therapy should be applied with caution, as it could increase the risk of POAG complications. It should be emphasized that the increased concentration of ALB and APCS in sclera extracts, in the absence of changes in hemoglobin content and without evidence of vascular

leakage in the scleral samples, indicates a specific association of these proteins with POAG.

Overall, in this study, we detected six proteins for the first time, namely, THBS4, ANGPTL7, ANXA2, VIM, ALB, and APCS, exhibiting specific changes in the sclera of patients with POAG. Importantly, different stages of glaucoma, including different IOP conditions, were characterized by specific patterns of these proteins, suggesting their contribution to abnormalities in scleral biochemistry and biomechanics, associated with the disease. Generally, the alterations may reflect pathological changes in glaucomatous sclera that relate mainly to the structure of the extracellular matrix, protein glycosylation, and calcium binding, and may involve fibroblast cytoskeleton regulation, as well as oxidative and inflammatory responses. Future studies are required to integrate this knowledge into the general understanding of POAG pathogenesis and to apply it to the development of an effective treatment for the disease.

APPENDIX 1. CHARACTERISTICS OF CONTROL AND POAG GROUPS.

To access the data, click or select the words "Appendix 1." * M, Myopia; H, Hyperopia; CHD, Coronary heart disease; HTN, Arterial hypertension; DM, Diabetes mellitus (type); ICH, Intracerebral hemorrhage.

APPENDIX 2. RESULTS OF MASS-SPECTROMETRY ANALYSIS OF SCLERAL PROTEINS.

To access the data, click or select the words "Appendix 2."

APPENDIX 3. IDENTIFICATION OF FIBRINOGEN ALPHA CHAIN IN SCLERAL EXTRACTS BY MALDI-TOF (MATRIX ASSISTED LASER DESORPTION IONIZATION-TIME OF FLIGHT [MALDI-TOF] MASS SPECTROMETRY [MS]) PEPTIDE MASS FINGERPRINTING.

To access the data, click or select the words "Appendix 3." The primary structure of human fibrinogen alpha chain (accession # P02671). The tryptic peptides identified by MS (red) and MS/MS (blue) analysis are indicated.

APPENDIX 4. THE WEIGHT FRACTIONS OF HEMOGLOBIN SUBUNITS ALPHA/BETA (HBA1/HBB) AND HISTONE H2A (HIST1H2AA) ESTIMATED FROM THE SDS-PAGE DATA OBTAINED FOR CONTROL INDIVIDUALS (100%) AND THE PATIENTS WITH STAGE IIIB POAG.

To access the data, click or select the words "Appendix 4."

APPENDIX 5. FUNCTIONAL BIOINFORMATICS ANALYSIS OF POAG-ASSOCIATED PROTEINS OF HUMAN SCLERA. THE RESULTS OF PATHWAYS ENRICHMENT ANALYSIS PERFORMED WITH ERICHR USING BIOPLANET 2019 (A) AND KEGG (KYOTO ENCYCLOPEDIA OF GENES AND GENOMES) 2019 (B). THE REVEALED TERMS ARE SORTED BY P-VALUE RANKING.

To access the data, click or select the words "Appendix 5."

APPENDIX 6. FUNCTIONAL BIOINFORMATICS ANALYSIS OF POAG-ASSOCIATED PROTEINS OF HUMAN SCLERA.

To access the data, click or select the words "Appendix 6." The results of disease/drugs enrichment analysis performed with Erichr using GWAS (genome-wide association studies) Catalog 2019 and UK Biobank GWAS v1. The revealed terms are denoted according their ID descriptions in UK biobank (https://biobank.ctsu.ox.ac.uk) and sorted by p-value ranking.

APPENDIX 7. STATISTICAL SIGNIFICANCE OF THE PROTEOMIC CHANGES IN POAG SCLERA.

To access the data, click or select the words "Appendix 7." * p-values according to two-tailed t-test in pairwise group comparisons.

ACKNOWLEGMENTS

This study was supported by the RUSSIAN SCIENCE FOUNDATION, grant number 16–15–00255.

REFERENCES

1. Razeghinejad MR, Myers JS, Katz LJ. Iatrogenic glaucoma secondary to medications. Am J Med 2011; 124:20-5. [PMID: 21092926].

2. Tham YC, Li X, Wong TY, Quigley HA, Aung T, Cheng CY. Global prevalence of glaucoma and projections of glaucoma burden through 2040: a systematic review and meta-analysis. Ophthalmology 2014; 121:2081-90. [PMID: 24974815].

3. Zernii EY, Baksheeva VE, Iomdina EN, Averina OA, Permyakov SE, Philippov PP, Zamyatnin AA, Senin II. Rabbit Models of Ocular Diseases: New Relevance for Classical Approaches. CNS Neurol Disord Drug Targets 2016; 15:267-91. [PMID: 26553163].
4. Overby DR, Clark AF. Animal models of glucocorticoid-induced glaucoma. Exp Eye Res 2015; 141:15-22. [PMID: 26051991].
5. Weinreb RN, Aung T, Medeiros FA. The pathophysiology and treatment of glaucoma: a review. JAMA 2014; 311:1901-11. [PMID: 24825645].
6. Morizane Y, Morimoto N, Fujiwara A, Kawasaki R, Yamashita H, Ogura Y, Shiraga F. Incidence and causes of visual impairment in Japan: the first nation-wide complete enumeration survey of newly certified visually impaired individuals. Jpn J Ophthalmol 2019; 63:26-33. [PMID: 30255397].
7. McMonnies CW. Glaucoma history and risk factors. J Optom 2017; 10:71-8. [PMID: 27025415].
8. Quigley HA, Vitale S. Models of open-angle glaucoma prevalence and incidence in the United States. Invest Ophthalmol Vis Sci 1997; 38:83-91. [PMID: 9008633].
9. McMonnies C. Reactive oxygen species, oxidative stress, glaucoma and hyperbaric oxygen therapy. J Optom 2018; 11:3-9. [PMID: 28760643].
10. Pinazo-Duran MD, Zanon-Moreno V, Garcia-Medina JJ, Gallego-Pinazo R. Evaluation of presumptive biomarkers of oxidative stress, immune response and apoptosis in primary open-angle glaucoma. Curr Opin Pharmacol 2013; 13:98-107. [PMID: 23142105].
11. Association between mitochondrial DNA damage and ocular blood flow in patients with glaucoma. Br J Ophthalmol 2019; 103:1060-5. [PMID: 30190366].
12. Fahy ET, Chrysostomou V, Crowston JG. Mini-Review: Impaired Axonal Transport and Glaucoma. Curr Eye Res 2016; 41:273-83. [PMID: 26125320].
13. Gauthier AC, Liu J. Neurodegeneration and Neuroprotection in Glaucoma. Yale J Biol Med 2016; 89:73-9. [PMID: 27505018].
14. Coudrillier B, Tian J, Alexander S, Myers KM, Quigley HA, Nguyen TD. Biomechanics of the human posterior sclera: age- and glaucoma-related changes measured using inflation testing. Invest Ophthalmol Vis Sci 2012; 53:1714-28. [PMID: 22395883].
15. Iomdina EN, Ignat'eva N, Danilov NA, Arutiunian LL, Kiseleva OA, Nazarenko LA. Biochemical, structural and biomechanical features of human scleral matrix in primary open-angle glaucoma . Vestn Oftalmol 2011; 127:10-4. [PMID: 22442986].
16. Sigal IA, Flanagan JG, Tertinegg I, Ethier CR. Finite element modeling of optic nerve head biomechanics. Invest Ophthalmol Vis Sci 2004; 45:4378-87. [PMID: 15557446].
17. Burgoyne CF, Downs JC, Bellezza AJ, Suh JK, Hart RT. The optic nerve head as a biomechanical structure: a new paradigm for understanding the role of IOP-related stress and strain in the pathophysiology of glaucomatous optic nerve head damage. Prog Retin Eye Res 2005; 24:39-73. [PMID: 15555526].
18. Boote C, Sigal IA, Grytz R, Hua Y, Nguyen TD, Girard MJA. Scleral structure and biomechanics. Prog Retin Eye Res 2020; 74:100773-[PMID: 31412277].
19. Coudrillier B, Pijanka J, Jefferys J, Sorensen T, Quigley HA, Boote C, Nguyen TD. Collagen structure and mechanical properties of the human sclera: analysis for the effects of age. J Biomech Eng 2015; 137:041006-[PMID: 25531905].
20. Jia X, Yu J, Liao SH, Duan XC. Biomechanics of the sclera and effects on intraocular pressure. Int J Ophthalmol 2016; 9:1824-31. [PMID: 28003987].
21. Sigal IA, Yang H, Roberts MD, Burgoyne CF, Downs JC. IOP-induced lamina cribrosa displacement and scleral canal expansion: an analysis of factor interactions using parameterized eye-specific models. Invest Ophthalmol Vis Sci 2011; 52:1896-907. [PMID: 20881292].
22. Sigal IA, Flanagan JG, Ethier CR. Factors influencing optic nerve head biomechanics. Invest Ophthalmol Vis Sci 2005; 46:4189-99. [PMID: 16249498].
23. Silver DM, Geyer O. Pressure-volume relation for the living human eye. Curr Eye Res 2000; 20:115-20. [PMID: 10617912].
24. Nguyen C, Cone FE, Nguyen TD, Coudrillier B, Pease ME, Steinhart MR, Oglesby EN, Jefferys JL, Quigley HA. Studies of scleral biomechanical behavior related to susceptibility for retinal ganglion cell loss in experimental mouse glaucoma. Invest Ophthalmol Vis Sci 2013; 54:1767-80. [PMID: 23404116].
25. Huang W, Fan Q, Wang W, Zhou M, Laties AM, Zhang X. Collagen: a potential factor involved in the pathogenesis of glaucoma. Med Sci Monit Basic Res 2013; 19:237-40. [PMID: 24002298].
26. Danilov NA, Ignatieva NY, Iomdina EN, Arutyunyan LL, Grokhovskaya TE, Lunin VV. Sclera of the glaucomatous eye: Physicochemical analysis. Biophysics (Oxf) 2011; 56:490-.
27. Cone-Kimball E, Nguyen C, Oglesby EN, Pease ME, Steinhart MR, Quigley HA. Scleral structural alterations associated with chronic experimental intraocular pressure elevation in mice. Mol Vis 2013; 19:2023-39. [PMID: 24146537].
28. Downs JC, Yang H, Girkin C, Sakata L, Bellezza A, Thompson H, Burgoyne CF. Three-dimensional histomorphometry of the normal and early glaucomatous monkey optic nerve head: neural canal and subarachnoid space architecture. Invest Ophthalmol Vis Sci 2007; 48:3195-208. [PMID: 17591889].
29. Girard MJ, Suh JK, Bottlang M, Burgoyne CF, Downs JC. Biomechanical changes in the sclera of monkey eyes exposed to chronic IOP elevations. Invest Ophthalmol Vis Sci 2011; 52:5656-69. [PMID: 21519033].
30. Girard MJ, Suh JK, Bottlang M, Burgoyne CF, Downs JC. Scleral biomechanics in the aging monkey eye. Invest Ophthalmol Vis Sci 2009; 50:5226-37. [PMID: 19494203].

31. Kasetti RB, Phan TN, Millar JC, Zode GS. Expression of Mutant Myocilin Induces Abnormal Intracellular Accumulation of Selected Extracellular Matrix Proteins in the Trabecular Meshwork. Invest Ophthalmol Vis Sci 2016; 57:6058-69. [PMID: 27820874].

32. Oglesby EN, Tezel G, Cone-Kimball E, Steinhart MR, Jefferys J, Pease ME, Quigley HA. Scleral fibroblast response to experimental glaucoma in mice. Mol Vis 2016; 22:82-99. [PMID: 26900327].

33. Finkelstein I, Trope GE, Basu PK, Hasany SM, Hunter WS. Quantitative analysis of collagen content and amino acids in trabecular meshwork. Br J Ophthalmol 1990; 74:280-2. [PMID: 2354136].

34. Micera A, Quaranta L, Esposito G, Floriani I, Pocobelli A, Sacca SC, Riva I, Manni G, Oddone F. Differential Protein Expression Profiles in Glaucomatous Trabecular Meshwork: An Evaluation Study on a Small Primary Open Angle Glaucoma Population. Adv Ther 2016; 33:252-67. [PMID: 26820987].

35. Funke S, Perumal N, Beck S, Gabel-Scheurich S, Schmelter C, Teister J, Gerbig C, Gramlich OW, Pfeiffer N, Grus FH. Glaucoma related Proteomic Alterations in Human Retina Samples. Sci Rep 2016; 6:29759-[PMID: 27425789].

36. Grigorieva JA, Dainiak MB, Katrukha AG, Muronetz VI. Antibodies to the nonnative forms of d-glyceraldehyde-3-phosphate dehydrogenase: identification, purification, and influence on the renaturation of the enzyme. Arch Biochem Biophys 1999; 369:252-60. [PMID: 10486144].

37. Egorov EA, Astakhov YS, Shuko AG. Glaucoma national guidelines. 1 ed. Moscow2008.

38. Fedorov SN, Kozlov VI. N.T. T. Non-penetrative deep sclerectomy in open-angle glaucoma. Ophthalmosurgery 1989; 3/4:52-5. .

39. Zamyatnin AA Jr, Solovyev AG, Bozhkov PV, Valkonen JP, Morozov SY, Savenkov EI. Assessment of the integral membrane protein topology in living cells. Plant J 2006; 46:145-54. [PMID: 16553902].

40. Awad D, Brueck T. Optimization of protein isolation by proteomic qualification from Cutaneotrichosporon oleaginosus. Anal Bioanal Chem 2020; 412:449-62. [PMID: 31797019].

41. Towbin H, Staehelin T, Gordon J. Electrophoretic transfer of proteins from polyacrylamide gels to nitrocellulose sheets: procedure and some applications. Proc Natl Acad Sci USA 1979; 76:4350-4. [PMID: 388439].

42. Adams JC, Lawler J. The thrombospondins. Cold Spring Harb Perspect Biol 2011; 3:a009712-[PMID: 21875984].

43. Peek R, Kammerer RA, Frank S, Otte-Holler I, Westphal JR. The angiopoietin-like factor cornea-derived transcript 6 is a putative morphogen for human cornea. J Biol Chem 2002; 277:686-93. [PMID: 11682471].

44. Sullivan-Mee M, Halverson K, Pensyl D, Colonna K, Gerhardt G, Chavez C. Anterior Scleral Rigidity in Primary Open-Angle Glaucoma. Invest Ophthalmol Vis Sci 2010; 51:5548-.

45. Zhang P, Karani R, Turner RL, Dufresne C, Ferri S, Van Eyk JE, Semba RD. The proteome of normal human retrobulbar optic nerve and sclera. Proteomics 2016; 16:2592-6. [PMID: 27538499].

46. Komai Y, Ushiki T. The three-dimensional organization of collagen fibrils in the human cornea and sclera. Invest Ophthalmol Vis Sci 1991; 32:2244-58. [PMID: 2071337].

47. Gopal S, Multhaupt HAB, Couchman JR. Calcium in Cell-Extracellular Matrix Interactions. Adv Exp Med Biol 2020; 1131:1079-102. [PMID: 31646546].

48. Bonnans C, Chou J, Werb Z. Remodelling the extracellular matrix in development and disease. Nat Rev Mol Cell Biol 2014; 15:786-801. [PMID: 25415508].

49. Vranka JA, Kelley MJ, Acott TS, Keller KE. Extracellular matrix in the trabecular meshwork: intraocular pressure regulation and dysregulation in glaucoma. Exp Eye Res 2015; 133:112-25. [PMID: 25819459].

50. Vranka JA, Staverosky JA, Reddy AP, Wilmarth PA, David LL, Acott TS, Russell P, Raghunathan VK. Biomechanical Rigidity and Quantitative Proteomics Analysis of Segmental Regions of the Trabecular Meshwork at Physiologic and Elevated Pressures. Invest Ophthalmol Vis Sci 2018; 59:246-59. [PMID: 29340639].

51. Si Z, Palkama A, Gebhardt BM, Velasquez D, Galeano MJ, Beuerman RW. Distribution of thrombospondin-4 in the bovine eye. Curr Eye Res 2003; 27:165-73. [PMID: 14562182].

52. Stenina-Adognravi O, Plow EF. Thrombospondin-4 in tissue remodeling. Matrix Biol 2019; 75–76:300-13. [PMID: 29138119].

53. Johnson M, Gong H, Freddo TF, Ritter N, Kamm R. Serum proteins and aqueous outflow resistance in bovine eyes. Invest Ophthalmol Vis Sci 1993; 34:3549-57. [PMID: 8258512].

54. Sit AJ, Gong H, Ritter N, Freddo TF, Kamm R, Johnson M. The role of soluble proteins in generating aqueous outflow resistance in the bovine and human eye. Exp Eye Res 1997; 64:813-21. [PMID: 9245912].

55. Si Z, Palkama A, Velasquez D, Gebhardt B, Beuerman R. Release of Thrombospondin-4 and Other Proteins from Outflow Pathways in the Human Eye. Invest Ophthalmol Vis Sci 2002; 43:3280-.

56. Pijanka JK, Kimball EC, Pease ME, Abass A, Sorensen T, Nguyen TD, Quigley HA, Boote C. Changes in scleral collagen organization in murine chronic experimental glaucoma. Invest Ophthalmol Vis Sci 2014; 55:6554-64. [PMID: 25228540].

57. Gebauer JM, Kohler A, Dietmar H, Gompert M, Neundorf I, Zaucke F, Koch M, Baumann U. COMP and TSP-4 interact specifically with the novel GXKGHR motif only found in fibrillar collagens. Sci Rep 2018; 8:17187-[PMID: 30464261].

58. Katoh Y, Katoh M. Comparative integromics on Angiopoietin family members. Int J Mol Med 2006; 17:1145-9. [PMID: 16685428].

59. Peek R, van Gelderen BE, Bruinenberg M, Kijlstra A. Molecular cloning of a new angiopoietinlike factor from the human cornea. Invest Ophthalmol Vis Sci 1998; 39:1782-8. [PMID: 9727400].

60. Kuchtey J, Kallberg ME, Gelatt KN, Rinkoski T, Komaromy AM, Kuchtey RW. Angiopoietin-like 7 secretion is induced by glaucoma stimuli and its concentration is elevated in glaucomatous aqueous humor. Invest Ophthalmol Vis Sci 2008; 49:3438-48. [PMID: 18421092].

61. Rozsa FW, Reed DM, Scott KM, Pawar H, Moroi SE, Kijek TG, Krafchak CM, Othman MI, Vollrath D, Elner VM, Richards JE. Gene expression profile of human trabecular meshwork cells in response to long-term dexamethasone exposure. Mol Vis 2006; 12:125-41. [PMID: 16541013].

62. Nehme A, Lobenhofer EK, Stamer WD, Edelman JL. Glucocorticoids with different chemical structures but similar glucocorticoid receptor potency regulate subsets of common and unique genes in human trabecular meshwork cells. BMC Med Genomics 2009; 2:58-[PMID: 19744340].

63. Comes N, Buie LK, Borras T. Evidence for a role of angiopoietin-like 7 (ANGPTL7) in extracellular matrix formation of the human trabecular meshwork: implications for glaucoma. Genes Cells 2011; 16:243-59. [PMID: 21199193].

64. Sienkiewicz AE, Rosenberg BN, Edwards G, Carreon TA, Bhattacharya SK. Aberrant glycosylation in the human trabecular meshwork. Proteomics Clin Appl 2014; 8:130-42. [PMID: 24458570].

65. Dismuke WM, Klingeborn M, Stamer WD. Mechanism of Fibronectin Binding to Human Trabecular Meshwork Exosomes and Its Modulation by Dexamethasone. PLoS One 2016; 11:e0165326-[PMID: 27783649].

66. Giovingo M, Nolan M, McCarty R, Pang IH, Clark AF, Beverley RM, Schwartz S, Stamer WD, Walker L, Grybauskas A, Skuran K, Kuprys PV, Yue BY, Knepper PA. sCD44 overexpression increases intraocular pressure and aqueous outflow resistance. Mol Vis 2013; 19:2151-64. [PMID: 24194636].

67. Bermudez JY, Montecchi-Palmer M, Mao W, Clark AF. Cross-linked actin networks (CLANs) in glaucoma. Exp Eye Res 2017; 159:16-22. [PMID: 28238754].

68. Mendez MG, Restle D, Janmey PA. Vimentin enhances cell elastic behavior and protects against compressive stress. Biophys J 2014; 107:314-23. [PMID: 25028873].

69. Bargagna-Mohan P, Deokule SP, Thompson K, Wizeman J, Srinivasan C, Vooturi S, Kompella UB, Mohan R. Withaferin A effectively targets soluble vimentin in the glaucoma filtration surgical model of fibrosis. PLoS One 2013; 8:e63881-[PMID: 23667686].

70. Mor-Vaknin N, Punturieri A, Sitwala K, Markovitz DM. Vimentin is secreted by activated macrophages. Nat Cell Biol 2003; 5:59-63. [PMID: 12483219].

71. Kaeslin MA, Killer HE, Fuhrer CA, Zeleny N, Huber AR, Neutzner A. Changes to the Aqueous Humor Proteome during Glaucoma. PLoS One 2016; 11:e0165314-[PMID: 27788204].

72. Carter-Dawson L, Zhang Y, Harwerth RS, Rojas R, Dash P, Zhao XC, WoldeMussie E, Ruiz G, Chuang A, Dubinsky WP, Redell JB. Elevated albumin in retinas of monkeys with experimental glaucoma. Invest Ophthalmol Vis Sci 2010; 51:952-9. [PMID: 19797225].

73. Zhao J, Wang S, Zhong W, Yang B, Sun L, Zheng Y. Oxidative stress in the trabecular meshwork Int J Mol Med 2016; 38:995-1002. Review[PMID: 27572245].

74. Cejka C, Cejkova J. Oxidative stress to the cornea, changes in corneal optical properties, and advances in treatment of corneal oxidative injuries. Oxid Med Cell Longev 2015; 2015:591530-[PMID: 25861412].

75. Wells AP, Garway-Heath DF, Poostchi A, Wong T, Chan KC, Sachdev N. Corneal hysteresis but not corneal thickness correlates with optic nerve surface compliance in glaucoma patients. Invest Ophthalmol Vis Sci 2008; 49:3262-8. [PMID: 18316697].

76. Uchida K, Himori N, Hashimoto K, Shiga Y, Tsuda S, Omodaka K, Nakazawa T. The association between oxidative stress and corneal hysteresis in patients with glaucoma. Sci Rep 2020; 10:545-[PMID: 31953470].

77. Duan X, Xue P, Wang N, Dong Z, Lu Q, Yang F. Proteomic analysis of aqueous humor from patients with primary open angle glaucoma. Mol Vis 2010; 16:2839-46. [PMID: 21203405].

78. Pepys MB, Baltz ML. Acute phase proteins with special reference to C-reactive protein and related proteins (pentaxins) and serum amyloid A protein. Adv Immunol 1983; 34:141-212. [PMID: 6356809].

79. Botto M, Hawkins PN, Bickerstaff MC, Herbert J, Bygrave AE, McBride A, Hutchinson WL, Tennent GA, Walport MJ, Pepys MB. Amyloid deposition is delayed in mice with targeted deletion of the serum amyloid P component gene. Nat Med 1997; 3:855-9. [PMID: 9256275].

80. Flight MH. Draining SAP to target Alzheimer's disease. Nat Rev Drug Discov 2009; 8:454-.

81. Li ZY, Streeten BW, Yohai N. Amyloid P protein in pseudoexfoliative fibrillopathy. Curr Eye Res 1989; 8:217-27. [PMID: 2714104].

82. Yin H, Chen L, Chen X, Liu X. Soluble amyloid beta oligomers may contribute to apoptosis of retinal ganglion cells in glaucoma. Med Hypotheses 2008; 71:77-80. [PMID: 18406539].

83. Guo L, Salt TE, Luong V, Wood N, Cheung W, Maass A, Ferrari G, Russo-Marie F, Sillito AM, Cheetham ME, Moss SE, Fitzke FW, Cordeiro MF. Targeting amyloid-beta in glaucoma treatment. Proc Natl Acad Sci USA 2007; 104:13444-9. [PMID: 17684098].

84. Bayer AU, Ferrari F, Erb C. High occurrence rate of glaucoma among patients with Alzheimer's disease. Eur Neurol 2002; 47:165-8. [PMID: 11914555].

85. Nucci C, Martucci A, Martorana A, Sancesario GM, Cerulli L. Glaucoma progression associated with altered cerebral spinal

fluid levels of amyloid beta and tau proteins. Clin Experiment Ophthalmol 2011; 39:279-81. [PMID: 20973903].

86. Goldblum D, Kipfer-Kauer A, Sarra GM, Wolf S, Frueh BE. Distribution of amyloid precursor protein and amyloid-beta immunoreactivity in DBA/2J glaucomatous mouse retinas. Invest Ophthalmol Vis Sci 2007; 48:5085-90. [PMID: 17962460].

87. McKinnon SJ, Lehman DM, Kerrigan-Baumrind LA, Merges CA, Pease ME, Kerrigan DF, Ransom NL, Tahzib NG, Reitsamer HA, Levkovitch-Verbin H, Quigley HA, Zack DJ. Caspase activation and amyloid precursor protein cleavage in rat ocular hypertension. Invest Ophthalmol Vis Sci 2002; 43:1077-87. [PMID: 11923249].

88. Gupta N, Fong J, Ang LC, Yucel YH. Retinal tau pathology in human glaucomas. Can J Ophthalmol 2008; 43:53-60. [PMID: 18219347].

89. Yoneda S, Hara H, Hirata A, Fukushima M, Inomata Y, Tanihara H. Vitreous fluid levels of beta-amyloid((1–42)) and tau in patients with retinal diseases. Jpn J Ophthalmol 2005; 49:106-8. [PMID: 15838725].

90. Wang WH, McNatt LG, Pang IH, Hellberg PE, Fingert JH, McCartney MD, Clark AF. Increased expression of serum amyloid A in glaucoma and its effect on intraocular pressure. Invest Ophthalmol Vis Sci 2008; 49:1916-23. [PMID: 18223246].

91. Inoue T, Kawaji T, Tanihara H. Elevated levels of multiple biomarkers of Alzheimer's disease in the aqueous humor of eyes with open-angle glaucoma. Invest Ophthalmol Vis Sci 2013; 54:5353-8. [PMID: 23860758].

92. Santhiago MR, Singh V, Barbosa FL, Agrawal V, Wilson SE. Monocyte development inhibitor PRM-151 decreases corneal myofibroblast generation in rabbits. Exp Eye Res 2011; 93:786-9. [PMID: 21933674].

93. Lockwood A, Brocchini S, Khaw PT. New developments in the pharmacological modulation of wound healing after glaucoma filtration surgery. Curr Opin Pharmacol 2013; 13:65-71. [PMID: 23153547].

94. Pilling D, Gomer RH. The Development of Serum Amyloid P as a Possible Therapeutic. Front Immunol 2018; 9:2328- [PMID: 30459752].

Articles are provided courtesy of Emory University and the Zhongshan Ophthalmic Center, Sun Yat-sen University, P.R. China. The print version of this article was created on 2 September 2020. This reflects all typographical corrections and errata to the article through that date. Details of any changes may be found in the online version of the article.